Inorg. Chem. **2005**, *44*, 7652–7660

An Electrochiroptical Molecular Switch: Mechanistic and Kinetic Studies

Homar S. Barcena,[†] Biao Liu,[‡] Michael V. Mirkin,*[,‡] and James W. Canary*[,†]

Department of Chemistry, New York University, New York, New York 10003, and Department of Chemistry and Biochemistry, Queens College—CUNY, Flushing, New York 11367

Received June 25, 2005

Previously, we reported the synthesis and preliminary characterization of Cu(I/II) complexes of *N*,*N*-bis(2-quinilylmethyl)-L-methionine (Zahn, S.; Canary, J. W. *Science* **2000**, *288*, 1404–7). The chemically oxidized and reduced forms of the complexes gave nearly mirror image circular dichroism (CD) spectra as a result of reorganization of the inner coordination sphere of the copper atom. The reorganization involved exchange of oxygen for sulfur in proceeding from the Cu(II) to Cu(I) oxidation state and corresponding ligand conformational changes required to accommodate this exchange. In this paper, we demonstrate that the complex can be triggered by electrochemical means. The electrochemical and stereochemical details of the redox-induced ligand reorganization were probed by independent synthesis of alternative chemical intermediates, CD spectroelectrochemistry, curve fitting of cyclic voltammograms, CD titration, and scanning electrochemical microscopy (SECM). A square-type mechanism was most consistent with the data: the Cu(II) complex is reduced followed by a ligand reorganization step to give the stable reduced form of the complex. The Cu(I) complex is then oxidized in a fast step followed by another ligand reorganization. A millisecond time scale rate was found by SECM for one of the key conformational conversion steps.

Introduction

Molecular switches offer potential applications in the field of molecular electronics and other visionary technologies in which triggered "on" and "off" states are addressed spectroscopically.[1−4] Several interesting chemical studies have been described in this context, including triggering by photochemical,[5−9] thermal,[10−13] chemical,[14,15] and electrochemical means.[16−20]

We have studied systems in which redox changes were coupled to chiroptical spectroscopic detection.[21−26] We described a system in which a one-electron redox change resulted in nearly mirror image circular dichroic spectra.[24] The system involves copper complexes of *N*,*N*-bis(2-quinolyl-

* To whom correspondence should be addressed. E-mail: Michael_Mirkin@qc.edu (M.V.M.); James.Canary@nyu.edu (J.W.C.).
[†] New York University.
[‡] Queens College—CUNY.

(1) Feringa, B. L.; Jager, W. F.; de Lange, B. *Tetrahedron* **1993**, *49*, 8267−310.
(2) Willner, I.; Rubin, S. *Angew. Chem., Int. Ed. Engl.* **1996**, *35*, 367−85.
(3) Balzani, V.; Credi, A.; Raymo, F. M.; Stoddart, J. F. *Angew. Chem., Int. Ed.* **2000**, *39*, 3348−3391.
(4) Feringa, B. L.; Koumura, N.; van Delden, R. A.; Ter Weil, M. K. *J. Appl. Phys. A* **2002**, *75*, 301−308.
(5) Spreitzer, H.; Daub, J. *Chem.*—Eur. J. **1996**, *2*, 1150−8.
(6) Feringa, B. L.; Jager, W. F.; de Lange, B. *J. Am. Chem. Soc.* **1991**, *113*, 5468−5470.
(7) Brouwer, A. M.; Frochot, C.; Gatti, F. G.; Leigh, D. A.; Mottier, L.; Paolucci, F.; Roffia, S.; Wurpel, G. W. *Science* **2001**, *291*, 2124−2128.
(8) de Jong, J. D.; Lucas, L. N.; Hania, R.; Pugzlys, A.; Kellogg, R. M.; Feringa, B. L.; Duppen, K.; van Esch, J. H. *Eur. J. Org. Chem.* **2003**, 1887−1893.
(9) De Waele, V.; Schmidhammer, U.; Mrozek, T.; Daub, J.; Riedle, E. *J. Am. Chem. Soc.* **2002**, *124*, 2438−2439.
(10) Gilat, S. L.; Kawai, S. H.; Lehn, J.-M. *Chem.*—Eur. J. **1995**, *1*, 275−84.
(11) Anelli, P. L.; Spencer, N.; Stoddart, J. F. *J. Am. Chem. Soc.* **1991**, *113*, 5131−5133.
(12) Anelli, P. L.; Ashton, P. R.; Ballardini, R.; Balzani, V.; Delgado, M.; Gandolfi, M. T.; Goodnow, T. T.; Kaifer, A. E.; Douglas, P.; Pietraszkiewwicz, M.; Prodi, L.; Reddington, M. V.; Slawin, A. M. Z.; Spencer, N.; Stoddart, J. F.; Vicent, C.; Williams, D. J. *J. Am. Chem. Soc.* **1992**, *114*, 193−218.
(13) Koumura, N.; Geertsema, E. M.; van Gelder, M. B.; Meetsma, A.; Feringa, B. L. *J. Am. Chem. Soc.* **2002**, *124*, 5037−5051.
(14) Lane, A. S.; Leigh, D. A.; Murphy, A. *J. Am. Chem. Soc.* **1997**, *119*, 11092−11093.
(15) Amendola, V.; Fabbrizzi, L.; Mangano, C.; Pallavicini, P. *Acc. Chem. Res.* **2001**, *34*, 488−493.
(16) Armaroli, N.; Balzani, V.; Collin, J.-P.; Gavina, P.; Sauvage, J.-P.; Ventura, B. *J. Am. Chem. Soc.* **1999**, *121*, 4397−408.
(17) Raehm, L.; Kern, J.-M.; Sauvage, J.-P. *Chem.—Eur. J.* **1999**, *5*, 3310−3317.
(18) Livoreil, A.; Dietrich-Buchecker, C. O.; Sauvage, J.-P. *J. Am. Chem. Soc.* **1994**, *116*, 9399−9400.
(19) Zellkovich, L.; Libman, J.; Shanzer, A. *Nature* **1995**, *374*, 790−792.
(20) Canevet, C.; Libman, J.; Shanzer, A. *Angew. Chem., Int. Ed. Engl.* **1996**, *35*, 2657−2660.

10.1021/ic051048m CCC: $30.25
Published on Web 09/17/2005

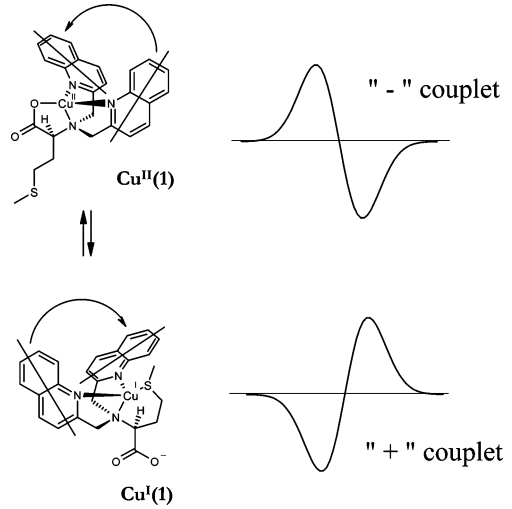

Figure 1. Inversion of helical chirality occurs upon chemical reduction and oxidation of copper, giving nearly mirror-image exciton-coupled circular dichroism spectra.

methyl)-(L)-methionine, where the Cu^{II} complex of **1** exhibits a negative couplet in the exciton-coupled circular dichroism (ECCD) spectra and chemical reduction of the Cu^{I} complex of **1** shows an ECCD sign inversion (Figure 1). The design of the ligand fashions a right-handed propeller when it is complexed with Cu^{II} and a left-handed propeller when it is complexed with Cu^{I}. A negative chiral orientation of the chromophores occurs when the metal center is coordinated to three nitrogen atoms and the carboxylate, giving rise to a (−)-couplet. Upon reduction with ascorbic acid, ligand reorganization occurs so that the dialkyl sulfide coordinates in place of the carboxylate, inverting the twist of the molecule to yield a (+)-couplet in the ECCD spectrum. The twist of the quinolyl chromophores is directed by the chiral center, as previously described in chiral tris((2-pyridyl)methyl)amine (TPA) complexes.[27]

The robustness of the system was demonstrated by performing several chemically induced cycles for the reduction and oxidation of the copper center, where very little signal hysteresis was observed using ascorbic acid and ammonium persulfate, respectively.[24]

Consideration of practical applications requires knowledge of mechanistic details concerning the redox cycle. Previously,[24] the square scheme shown in Scheme 1 was proposed. This mechanism was based on known structures **O** and **R**, while intermediates **P** and **Q** were assumed. The gross features of Scheme 1 are supported by literature precedent, and copper centers are well-known to exhibit such mechanisms.[28] While it is believed that complexes in the Cu^{I} state

Scheme 1. Illustration of the Proposed Square Mechanism[a]

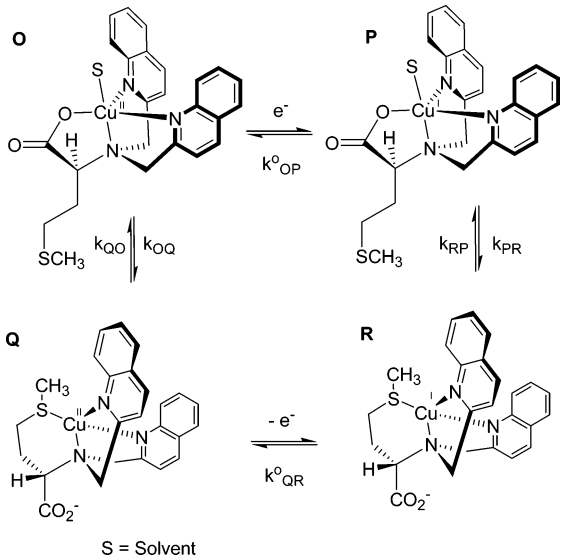

[a] Electron-induced ligand reorganization results in an inversion of the chromophore orientation ($k^{o}_{OP,QR}$ = rate of electron transfer, $k_{PR,OQ}$ = forward rate of reaction, $k_{RP,QO}$ = reverse rate of reaction).

are stabilized by sulfur-containing ligands and carboxylate-containing ligands stabilize the Cu^{II} state,[29,30] Rorabacher[31] has shown that the Cu^{I} state has no preference for the type of donor atom, but rather the Cu^{II} state is destabilized by sulfur atoms. Reduction of the Cu(II) complex **O** gives species **P**, which undergoes a ligand reorganization to give **R**. Thus, the stable species **O** and **R** are derived from electron-induced reorganization of the ligand via the metastable intermediates **P** and **Q**. This mechanism is similar to ones proposed for nitrogen- and sulfur-containing ligands that are used in studies involving electron-transfer kinetics in complexes that mimic blue copper proteins, where data were obtained using absorbance,[31−35] fast-scan cyclic voltammetry (CV),[36,37] and NMR experiments.[38]

However, several questions remained about this mechanism. One fundamental question regards the oxidation step with ammonium persulfate. This reagent is capable of oxidizing sulfur atoms[39] and might oxidize the methionine

(21) Belle, C.; Pierre, J.-L.; Saint-Aman, E. *New. J. Chem.* **1998**, *22*, 1399−1402.
(22) Kalny, D.; Mourad, E.; Tamar, M.; Vaskevich, A.; Rubinstein, I.; Shanzer, A.; Albrecht-Gary, A.-M. *Chem. Commun.* **2002**, *12*, 1426−1427.
(23) Zahn, S.; Canary, J. W. *Angew. Chem., Int. Ed.* **1998**, *37*, 305−307.
(24) Zahn, S.; Canary, J. W. *Science* **2000**, *288*, 1404−1407.
(25) Zahn, S.; Canary, J. W. *J. Am. Chem. Soc.* **2002**, *124*, 9204−9211.
(26) Barcena, H.; Holmes, A. E.; Zahn, S.; Canary, J. W. *Org. Lett.* **2003**, *5*, 709−711.
(27) Castagnetto, J. M.; Xu, X.; Berova, N. D.; Canary, J. W. *Chirality* **1997**, *9*, 616−22.
(28) Rorabacher, D. B. *Chem. Rev.* **2004**, *104*, 651−697.
(29) Lippard, S. J.; Berg, J. M. *Principles of Bioinorganic Chemistry*; University Science Books: Mill Valley, CA, 1994.
(30) Tyeklar, Z.; Karlin, K. D. *Bioinorganic Chemistry of Copper*; VCH: New York, 1993.
(31) Wijetunge, P.; Kulatilleke, C. P.; Dressel, L. T.; Heeg, M. J.; Ochrymowycz, L. A.; Rorabacher, D. B. *Inorg. Chem.* **2000**, *39*, 2897−2905.
(32) Koshino, N.; Kuchiyama, Y.; Funahashi, S.; Tagaki, H., D. *Chem. Phys. Lett.* **1999**, *306*, 291−296.
(33) Koshino, N.; Kuchiyama, Y.; Ozaki, H.; Funahashi, S.; Tagaki, H. D. *Inorg. Chem.* **1999**, *38*, 3352−3360.
(34) Dunn, B. C.; Wijetunge, P.; Vyvyan, J. R.; Howard, T. A.; Grall, A. J.; Ochrymowycz, L. A.; Rorabacher, D. B. *Inorg. Chem.* **1997**, *36*, 4484−4489.
(35) Dunn, B. C.; Ochrymowycz, L. A.; Rorabacher, D. B. *Inorg. Chem.* **1997**, *36*, 3253−3257.
(36) Robandt, P. V.; Schroeder, R. R.; Rorabacher, D. B. *Inorg. Chem.* **1993**, *32*, 3957−3963.
(37) Villeneuve, N. M.; Schroeder, R. R.; Ochrymowycz, L. A.; Rorabacher, D. B. *Inorg. Chem.* **1997**, *36*, 4475−4483.
(38) Flanagan, S.; Dong, J.; Haller, K.; Wang, S.; Scheidt, R. W.; Scott, R. A.; Webb, T. R.; Stanbury, D. M.; Wilson, L. J. *J. Am. Chem. Soc.* **1997**, *119*, 8857−8868.

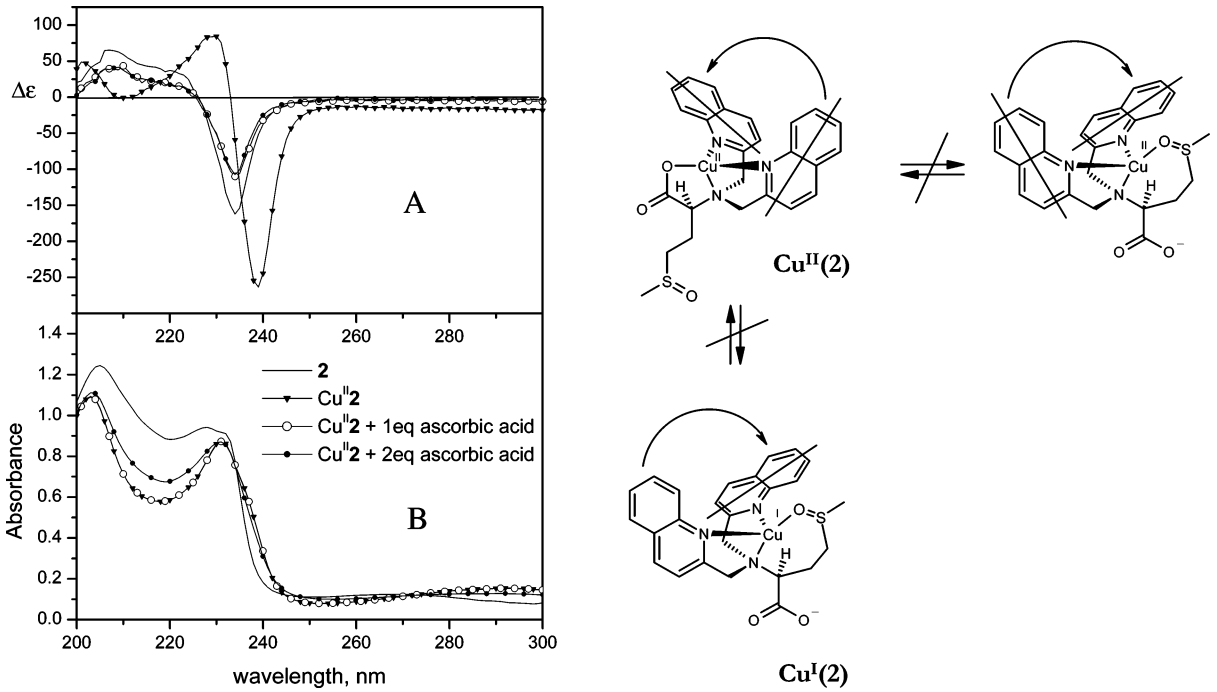

Figure 2. CD (A) and UV spectra (B) of the sulfoxide analogue Cu^{II}(**2**) in acetonitrile (0.1 mM). The disappearance of ECCD in Cu^{II}(**2**) upon addition of ascorbic acid indicates that the sulfoxide does not bind to the metal.

side chain to sulfoxide. Second, while Scheme 1 indicates oxidation/reduction occurring (**O** → **P**) prior to ligand reorganization (**P** → **R**), we sought to exclude other possibilities experimentally such as ligand reorganization (**O** → **Q**) prior to redox reaction (**Q** → **R**). Finally, we were interested in obtaining rate information about the switching events, as rate properties will strongly affect any potential applications of the chemistry.

Results and Discussion

Sulfoxide Independent Synthesis and Characterization. Ammonium persulfate was employed as the chemical oxidant in prior studies.[23−25] This reagent is capable of oxidizing the sulfur atom[39] which would be irreversible and prevent cycling. However, strong reversibility was observed with several chemical oxidation/reduction cycles with little hysteresis,[23,24] but it seemed appropriate to look more carefully at this possibility prior to mechanistic studies. This question was examined initially by measuring mass spectra of ligand and complexes after reaction with persulfate. While this reagent oxidized the ligand, several attempts failed to show clearly whether oxidation occurred under the conditions of the redox cycling reactions.

The sulfoxide **2** was synthesized directly by oxidizing the methyl ester of *N*,*N*-bis(2-quinaldyl)methionine[40] using bromine and water in methylene chloride[41] in 67% yield. Subsequent saponification with lithium hydroxide solution afforded the ligand in 32% yield. NMR data suggested the product was a mixture of diastereomers.

The circular dichroism spectrum of the free ligand (Figure 2A) showed a negative Cotton effect at 234 nm, almost coincident to the λ_{max} at 231 nm (Figure 2B). Complexation with Cu^{II} resulted in an increase in amplitude and an appearance of a negative bisignate curve with inflection point at 233 nm; these features are characteristic of exciton coupling.[42] Upon reduction of the metal with ascorbic acid, the signal diminished in amplitude and resembled the spectrum of the free ligand. The disappearance of ECCD in comparison to the reduction of the parent complex Cu^{II}(**1**), which showed a positive ECCD, indicates that the sulfoxide does not bind to either Cu^{II} or Cu^{I}. If the sulfoxide arm were coordinating to cuprous ion, one would expect to see some type of ECCD spectrum with positive Cotton effect near 240 nm.

CD Spectroelectrochemistry. Controlled potential coulometry was performed on Cu^{II}(**1**), which, under our experimental conditions, showed a $\Delta\epsilon = 200$ (Figure 3). Upon completion of electrolysis, the solution color changed from blue to yellow, indicative of the reduction that had taken place. The CD of the resultant solution of Cu^{I}(**1**) showed a small but positive couplet ($\Delta\epsilon = 8$), whereas the UV was similar to that observed by direct preparation or chemical reduction.[24]

The CD and the UV spectra obtained for Cu^{II}(**1**) in acetonitrile with TBAP are almost identical with the spectra obtained without the added electrolyte (negative couplet with $\Delta\epsilon = 220$; $\lambda_{max} = 231$ nm). Upon chemical reduction to Cu^{I}(**1**) with ascorbic acid, the opposite couplet was observed ($\Delta\epsilon = 115$; $\lambda_{max} = 230$ nm). These control studies indicate

(39) Kim, Y. H. In *Sulfur and Phosphorus Peroxides*; Ando, W., Ed.; John Wiley and Sons: New York, 1992; pp 387−391.
(40) Zahn, S. Electron Driven Chiroptical Materials. Ph.D. Dissertation, New York University: New York, 2000; p 235.
(41) Bravo, A.; Dordi, B.; Fontana, F.; Minisci, F. *J. Org. Chem.* **2001**, *66*, 3232−3234.
(42) Nakanishi, K.; Berova, N.; Woody, R. *Circular Dichroism: Principles and Applications*, 2nd ed.; Wiley-VCH: New York, 2000.

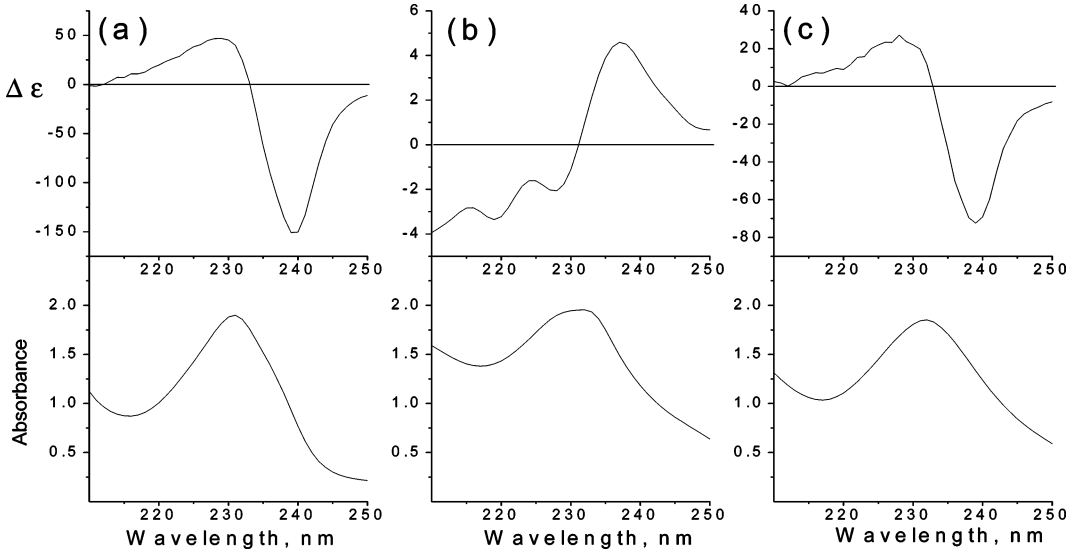

Figure 3. CD/UV spectroelectrochemistry of Cu^{II}(**1**) (a) and the electrolysis product at −1 V, Cu^{I}(**1**) (b). Subsequent oxidation to Cu^{II}(**1**) at +1 V resulted in a diminished but positive couplet (c).

that the presence of TBAP does not significantly affect the chiroptical signal in both copper states.

The reason for the loss in signal amplitude in Cu^{I}(**1**) compared with generation of Cu^{I}(**1**) by other methods is not clear. The reoxidation of Cu^{I}(**1**) is shown in Figure 3c, which shows a diminished signal as compared to the starting solution. One difference between the chemical and electrochemical reduction schemes is that byproducts of the ascorbate reduction[43] include materials that may influence the spectra. Although the amplitude is smaller, the shape and the signature of the ECCD are similar to that of the starting material (Figure 3a). The UV spectra within the redox cycle consistently show the maximum at 231 nm, with comparable amplitudes; this provides qualitative evidence that the molecular switch survives the experiment.

Cyclic Voltammetry. Cyclic voltammetry (CV) and digital simulation used to evaluate the mechanism and explain the switching behavior observed by CD spectroscopy upon chemical reduction and oxidation.[44] The square scheme model (Scheme 1) suggests that the ligand reorganizations occur after electron transfer (EC mechanism) for the reduction cycle, and such processes can be assessed by CV. Establishing that conformational control around the metal center proceeds in a unidirectional fashion is desirable to ensure that the switching input generates the chiroptical output. Biological molecular switches have been speculated to employ similar conformational control to prevent undesired reaction pathways.[45]

Numerous parameters were first examined to determine optimum conditions that would yield voltammograms suitable for data fitting. These included glassy-carbon, platinum, and gold working electrodes, silver wire and silver chloride reference electrodes, tetrabutylammonium hexafluorophosphate or tetrafluoroborate electrolytes, and nitrobenzene and dichloromethane as solvents.

Importantly, the experimental voltammograms (Figure 4) could not be fit to the theory for slow heterogeneous kinetics without coupled homogeneous kinetics in solution. Under

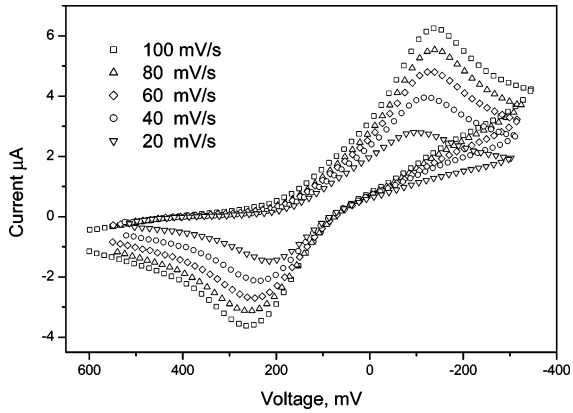

Figure 4. Cyclic voltammograms of 1 mM Cu^{II}(**1**) at different scan rates on glassy carbon electrode (0.070 69 cm^2) and 0.1 M TBAP electrolyte in acetonitrile.

Table 1. Potential Peaks for Cu^{II}(**1**) at Different Scan Rates (Reference: $Ag/AgClO_4$ in CH_3CN)

ν (mV/s)	$E_{p,red}$ (mV)	$E_{p,ox}$ (mV)	ΔE_p (mV)	$(E_{p,red} + E_{p,ox})/2$ (mV)
100	−147	260	407	56
80	−143	261	404	59
60	−134	247	381	56
40	−128	240	368	56
20	−109	207	316	49

slow-scan conditions, we observed two widely separated peaks, indicative of two electrochemical events. First, we detect the reduction of **O** to **P** (the peak potential, $E_{p,red} \sim -140$ mV), which according to our hypothesis leads to a fast ligand reorganization **P** → **R** that is not detected at the CV time scale. Reoxidation of **R** to **Q** is then observed ($E_{p,ox} \sim 250$ mV) with ensuing **Q** → **O** reorganization. The large separation between the peaks (ΔE_p in Table 1) supports the mechanism in Scheme 1, since the switching event requires ligand reorganization from a five-membered ring chelate of

(43) Taqui, M. M.; Martell, A. E. *J. Am. Chem. Soc.* **1967**, *89*, 7104−7111.
(44) Rudolph, M.; Reddy, D. P.; Feldberg, S. W. *Anal. Chem.* **1994**, *66*, 589 A − 600 A.
(45) Pratt, J. M. *J. Inorg. Biochem.* **1986**, *28*, 145−153.

Table 2. Simulated CV Parameters for $Cu^{II}(1)$[a]

υ (mV/s)	$E°_{red}$ (mV)	$k°_{red}$ (cm s^{-1})	K_{PR}	$E°_{ox}$ (mV)	$k°_{ox}$ (cm s^{-1})	K_{QO}
100	67.7	0.000 18	54.3	430	0.021	2.42×10^4
80	57.1	0.000 14	45.2	390	0.012	9.29×10^3
60	60.1	0.000 17	38.1	408	0.012	1.99×10^4
40	57.7	0.000 21	25.4	399	0.029	2.27×10^5
20	37.2	0.000 26	22.4	390	0.032	4.14×10^4

[a] $E_{red,ox}$ = peak potential, $k°_{red,ox}$ = rate of electron transfer, D = diffusion rates for each species, $K_{PR,QO}$ = equilibrium constant, K_{PR} = [**R**]/[**P**], and K_{QO} = [**O**]/[**Q**]; **O**, **P**, **Q**, and **R** refer to species illustrated in Scheme 1.

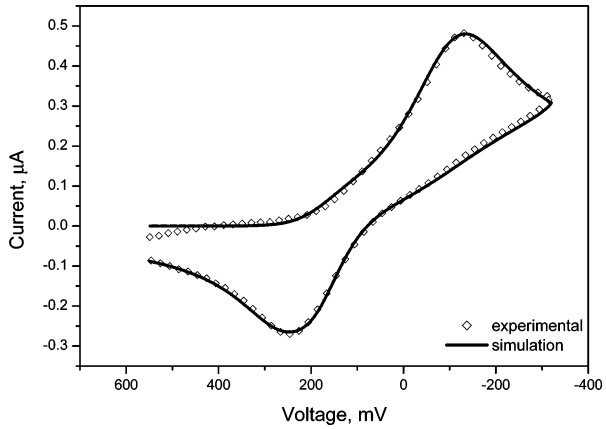

Figure 5. Experimental and simulated voltammograms for **1** at scan rate 60 mV s^{-1}.

the carboxylate with Cu^{II} to a six-membered ring chelate of the thioether group with Cu^{I}. This also excludes the possibility of ligand reorganization (**O** → **Q**) prior to electron transfer (**Q** → **R**), since this would show a reversible type voltammogram.

The midpoint potential of the system, $(E_{p,red} + E_{p,ox})/2$, correlates with previously listed redox potentials for $Cu^{II/I}$ systems that have nitrogen, sulfur, and oxygen atoms coordinated to the metal.[38] For instance, ligands which have a donor atom set (DAS) of N_5 have negative potentials, while increasing the sulfur or oxygen content of the DAS promotes an increase in the midpoint potential.[38] Our values are consistent with published data on the basis of the number of nitrogen, sulfur, and oxygen atoms in our DAS. Thus, the stabilization imbued by the carboxylate to Cu^{II} and by the thioether to Cu^{I} is evident from the data in Table 1. Furthermore, the widely separated redox potentials are consistent with large structural reorganization, as observed for other systems with coordination number variance or inversion at the sulfur.[38,46]

The summary of the simulation parameters is listed in Table 2, and an example of the fit quality is given in Figure 5. One should notice that K_{QO} is significantly larger than K_{PR}, indicating that species **P** is relatively more stable than **Q**. This is not surprising, since Cu^{II} is generally thought to be more sensitive toward variance in coordination sphere than Cu^{I}.[47] These results further validate the directionality of the square scheme mechanism, since the alternative where ligand reorganization occurs prior to electron transfer (**O** → **Q**, **Q** + e^- → **R**) is less likely if intermediate **Q** is much less stable than intermediate **P**. A parallel comparison can be made with simulation data from several complexes which exhibit similar gating directionality. For $Cu^{II/I}$ macrocyclic thioether complexes, the equilibrium constant for **R** → **P** transformation (K_{RP}) was from 1 to 4 orders of magnitude greater than **O** → **Q** (K_{OQ});[37] for these complexes, it follows that **P** is more stable than **Q**. While Rorabacher has suggested that dual pathway mechanisms may be common to all $Cu^{II/I}$ systems, when **P** is more stable than **Q**, the gating is in the direction described here.[48] Theoretical treatment of the square mechanism anticipates that "gated" or "directional" electron transfer occurs when formation of one of the high-energy intermediates is faster (i.e., **P** is formed faster than **Q**).[49,50]

It should be noted that certain processes in Scheme 1 may involve more than one step,[31,51] such as P → R which represents both the reorganization of the tetradentate ligand and probable loss of coordinated solvent. Such phenomena were not included in the model but may be reflected in the variation of certain constants at variable scan rates. Previous studies involving the square mechanism[37,52] were carried out under such conditions that the chemical processes competed with the electron transfer step on the electrode. When the scan rate was sufficiently fast to detect the chemical process **P** → **R** and **Q** → **O**, two additional peaks appeared in the voltammogram.[51] This behavior enabled researchers to quantify the rate of conformational change in these complexes. In kinetic studies involving copper complexes of macrocyclic tetrathioethers, only limiting estimates of the conformational rate constants were obtained in the absence of conformational gating.[35] Because of mass transfer limitations, we were unable to detect the metastable intermediates **P** and **Q** or to measure the rates of related homogeneous chemical reactions from slow scan voltammograms. Therefore, Table 2 does not contain the homogeneous rate constant values. The votammogram shape depended strongly on the value of each parameter shown in that table. Attempts to use fast scan voltammetry to measure kinetics of homogeneous reactions involved in redox switching process (Scheme 1) were unsuccessful. Fast scan cyclic voltammograms are strongly affected by very small amount of adsorption of reactant or intermediate.[53] Measurements taken at low temperatures (−45 °C) did not show the appearance of a new peak, as opposed to previous studies involving cyclic thiaethers.[37,52]

(46) Ramalingam, B.; Mallayan, P.; Gopalan, R. S. *Inorg. Chem.* **2001**, *40*, 2246−2255.
(47) Ambundo, E. A.; Deydier, M.-V.; Grall, A. J.; Aguera-Vega, N.; Dressel, L. T.; Cooper, T. H.; Heeg, M. J.; Ochrymowycz, L. A.; Rorabacher, D. B. *Inorg. Chem.* **1999**, *38*, 4233−4242.
(48) Meagher, N. E.; Juntunen, K. L.; Heeg, M. J.; Salhi, C. A.; Dunn, B. C.; Ochrymowycz, L. A.; Rorabacher, D. B. *Inorg. Chem.* **1994**, *33*, 670−79.
(49) Hoffman, B. M.; Ratner, M. A. *J. Am. Chem. Soc.* **1987**, *109*, 6237−6243.
(50) Brunschwig, B. S.; Sutin, N. *J. Am. Chem. Soc.* **1989**, *111*, 7454−7465.
(51) Evans, D. H. *Chem. Rev.* **1990**, *90*, 743.
(52) Bernardo, M. M.; Robandt, P. V.; Schroeder, R. R.; Rorabacher, D. B. *J. Am. Chem. Soc.* **1989**, *111*, 1224−1231.
(53) Bard, A.; Faulkner, L. R. *Electrochemical Methods: Fundamentals and Applications*, 2nd ed.; Wiley & Sons: New York, 2001; p 569.

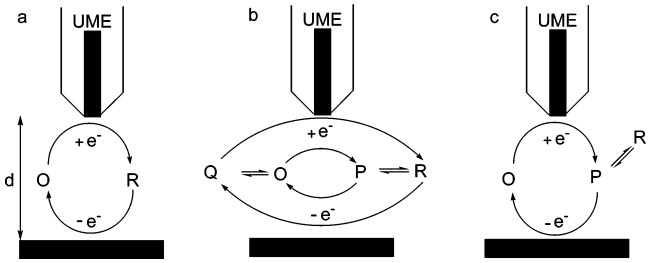

Figure 6. SECM schematic showing tip feedback collection mode for a simple redox reaction (a), complete square mechanism (b), and simplified square mechanism (c).

SECM Measurements of Switching Kinetics. Unlike CV, scanning electrochemical microscopy (SECM), offers much higher mass transfer rates under steady-state conditions. It was used previously to detect short-lived intermediates in very fast homogeneous reactions coupled to heterogeneous electron transfer.[54] Kinetic information can be extracted from steady-state SECM data when the system behavior is complicated by adsorption and the voltammetric response is not perfect.[55]

In feedback mode, the analyte is cycled between a movable ultramicroelectrode (UME) tip and a conductive substrate. When the distance between the tip and the substrate is large, a well-defined steady-state current ($i_{T,\infty}$) is detected at the tip, due to the diffusion-controlled reduction of analyte (**O**). When the tip is brought closer to the substrate, the reduced species (**R**) can be oxidized back to **O (**Figure 6a) and the tip current becomes greater than $i_{T,\infty}$.

For the square mechanism (Figure 6b), the presence of four different species that could undergo electrochemical and conformational changes dramatically complicates the experiment. Using SECM, the complicated kinetic analysis of a square mechanism can be simplified by independently probing its two "halves" (Figure 6c). For example, if the substrate potential is sufficiently positive to oxidize **P** but not **R**, the overall SECM process is reduced to the EC mechanism:

$$\mathbf{O} + e^- \rightarrow \mathbf{P}\ (\text{tip}) \qquad (1)$$

$$\mathbf{P} \rightarrow \mathbf{O} + e^-\ (\text{substrate}) \qquad (2)$$

$$\mathbf{P} \xrightarrow{k_{PR}} \mathbf{R}\ (\text{interelectrode gap}) \qquad (3)$$

Because $K_{PR} \gg 1$ (Table 2), the rate of reaction 3 in reverse direction was neglected in our treatment. The rate of this process, which represents the ligand reorganization, could be extracted from the SECM current vs distance (approach) curves.[56] Study of the oxidation process was frustrated by the air sensitivity of Cu^I and is not reported.

The approach curves shown in Figure 7 demonstrate that the process is controlled by finite kinetics; i.e., the measured tip current is significantly higher than the theoretical curve calculated for an insulating substrate (lower dashed line) and lower than the current expected for a diffusion-controlled process (upper dashed line). To ensure that the rate-determining step is a homogeneous rather than heterogeneous reaction, we obtained approach curves at different substrate potentials (E_S). Clearly the curves obtained at E_S = 0.30 V (triangles) and 0.42 V (circles) are practically identical. This indicates that the substrate potential does not affect the rate of the overall mediator regeneration process, which is limited by homogeneous ligand rearrangement reaction.

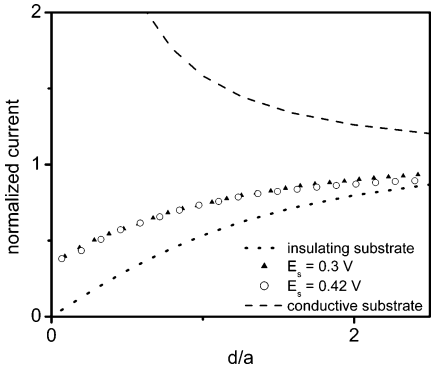

Figure 7. Normalized tip current vs distance curves for redox switching process (reactions 1−3). The acetonitrile solution contained 1 mM of Cu^{II}(**1**) and 100 mM tetrabutylammonium perchlorate. Experimental curves were obtained at E_S = 0.3 V (triangles) and 0.42 V (circles). Dashed lines represent the theory for an SECM diffusion-controlled process with a conductive (upper curve) and insulating (lower curve) substrate.[57,58] The tip was a 5.5-μm radius carbon fiber electrode biased at −0.5 V vs $Ag/AgClO_4$ reference electrode.

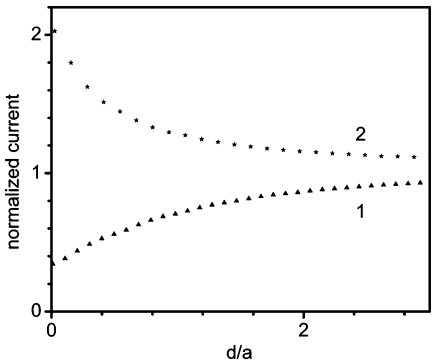

Figure 8. Comparison of the current−distance curves measured at different substrate potentials. E_S = 0.3 V (1) and 0.9 V (2). For other parameters, see Figure 7.

Both substrate potentials in Figure 7 (i.e., 0.30 and 0.42 V) were chosen such that the oxidation of species **P** was diffusion controlled but no oxidation of species **R** was possible (Figure 6c). Since homogeneous reaction (**P** → **R**) is pretty fast, a relatively small fraction of mediator species was reoxidized at the substrate and the feedback current in Figure 7 is low. In contrast, at a more positive E_S value (e.g., 0.9 V), simultaneous oxidation of both **P** and **R** at the substrate produces a much higher feedback current (compare curves 1 and 2 in Figure 8).

A previously developed approach to determination of k_{PR} by SECM is based on an analytical approximation relating the dimensionless parameter ($\kappa = k_{PR}d^2/D$) to collection efficiency ($x = I_S/I_T$):[59]

(54) Unwin, P. R. In *Scanning Electrochemical Microscopy*; Bard, A. J., Mirkin, M. V., Eds.; Marcel Dekker: New York, 2001; pp 241−298.
(55) Mirkin, M. V.; Yang, H.; Bard, A. J. *J. Electrochem. Soc.* **1992**, *139*, 2212−17.
(56) Unwin, P. R.; Bard, A. J. *J. Phys. Chem.* **1991**, *95*, 7814.

$$\kappa = F(x) = 5.608 + 9.347\exp(-7.527x) - 7.616\exp(-0.307/x) \quad (4)$$

Here d is the distance between the tip and the substrate and I_S and I_T are substrate and tip currents, respectively, normalized by the tip current at infinite tip−substrate separation (i.e., $I_T = i_T/i_{T,\infty}$ and $I_S = i_S/i_{T,\infty}$). The collection efficiency values most suitable for determination of k_{PR} are those between about 0.2 and 0.8.

To find the collection efficiency experimentally, one has to measure both I_S and I_T values as a function of d. This is possible if substrate current is produced only by oxidation/reduction of species generated at the tip (i.e., $I_S = 0$ at large d). The substrate current could not be measured accurately. In this case, the collection efficiency can be calculated from the experimental tip current vs distance curve:[59]

$$I_S/I_T = (1 - I_T^{ins}/I_T)/[1 - f(L)] \quad (5)$$

Here $L = d/a$ is the tip/substrate distance normalized by the tip radius, $f(L) = I_T^{ins}/I_T^{cond}$, and I_T^{ins} and I_T^{cond} are the tip currents with a conductive and an insulating substrate, respectively,[58]

$$I_T^{cond} = 0.78377/L + 0.3315\exp(-1.0672/L) + 0.68 \quad (6)$$

$$I_T^{ins} = 1/(0.15 + 1.5358/L + 0.58\exp(-1.14/L) + 0.0908\exp[(L - 6.3)/(1.017L)]) \quad (7)$$

The rate constant of the ligand rearrangement reaction 3, $k_{PR} = 25\ s^{-1}$, was determined from the best fit of the experimental collection efficiency values to eq 4 (Figure 9). The accuracy of the result may not be very high because of additional complexity of the studied system, but it provides a reliable estimate of the half-life (ln 2/k) for the **P** → **R** ligand rearrangement, which appears to be ∼25 ms.

Circular Dichroic Spectroscopy Titration. To eliminate the possibility of hysteresis due to Cu^I decomplexation from the ligand, and thus altering the switching rate determined from SECM, the binding constant of the ligand needed to be determined. We paid close attention to Cu^I, since acetonitrile tends to form air-stable complexes with this oxidation state of the metal.

One of the advantages of our chiroptical switch is that the amplitude of the CD signal is large due to exciton coupling. Thus, we are able to detect a change in ellipticity ($\Delta\theta$) even at low concentrations, ideal for stability constant determination. Titration of Cu(I) to a ligand solution shows gradual increase of $\Delta\theta$. Nonlinear least-squares fitting of the data afforded the stability constant using the following mathematical treatment:

$$\Delta\Delta\theta = \{\alpha([L] + [Cu^I] + 1/K_s) + \sqrt{\alpha^2([L] + [Cu^I] + 1/K_s)^2 - 4\alpha^2[L][Cu^I]}\}/2$$

Here $\Delta\Delta\theta$ is the change in ellipticity, α is a proportionality coefficient, and K_s is the complex stability constant.[60] Figure 10 shows the resultant fit, which still shows saturation at 1:1 ligand:copper; this gives an upper limit approximation of $K_s = 4 \times 10^6$ and $\alpha = 2 \times 10^4$. The α value measures the degree of conformational change upon complexation, and the value obtained conforms reasonably with the ones determined from chiral induction upon guest complexation in cyclodextrins.

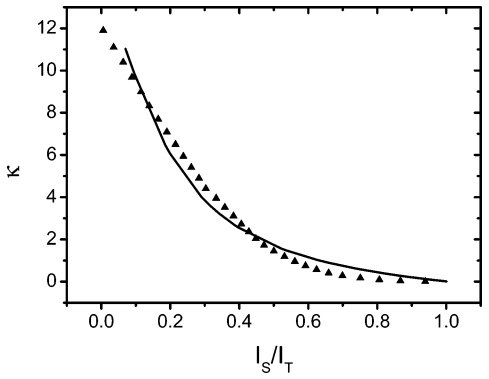

Figure 9. Kinetic parameter κ as a function of the calculated collection efficiency. Triangles were calculated from experimental data in Figure 7 with $\kappa = 3.0$, and the solid line was obtained from eq 4. $E_S = 0.3$ V. Other experimental conditions are as in Figure 7.

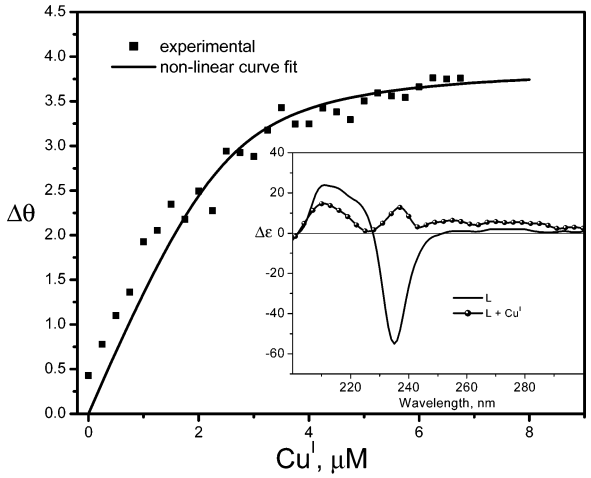

Figure 10. CD titration studies of 15 μM Cu^I to 2.5 μM **1**. Inset: CD spectra of ligand before and after titration.

Conclusions

The unique electrochiroptical switching behavior of our system was examined using a variety of techniques. CD spectroelectrochemistry demonstrated the ability to interconvert the two states without chemical reagents, as would greatly benefit device development. Synthesis of the sulfoxide of the ligand and demonstration of its inability to show chiroptical inversion eliminated the possibility that chemistry at sulfur is responsible for the chiroptical inversion. Cyclic voltammetry measurements substantiated the square mechanism cycle as the most likely mechanism, and curve-fitting

(57) Kwak, J.; Bard, A. J. *Anal. Chem.* **1989**, *61*, 1794−9.
(58) Mirkin, M. V.; Fan, F. R. F.; Bard, A. J. *J. Electroanal. Chem.* **1992**, *328*, 47−62.
(59) Treichel, D. A.; Mirkin, M. A.; Bard, A. J. *J. Phys. Chem.* **1994**, *98*, 5751−5757.
(60) Inoue, Y.; Yamamoto, K.; Wada, T.; Everitt, S.; Gao, X.-M.; Hou, Z.-J.; Tong, L.-H.; Jiang, S.-K.; Wu, H.-M. *J. Chem. Soc., Perkin Trans. 2* **1998**, 1807−1816.

established the likely sequence of steps. SECM experiments were supportive of the proposed mechanism and provided insight into the likely time scale of at least one of the conformational reorganization events in the cycle. These studies begin to provide a more detailed picture of the mechanism of this interesting system, although further studies will be required, perhaps using NMR or photochemical techniques, with a redesigned system that allow such investigations.

Experimental Section

Chemicals. The complex Cu^{II}(**1**)ClO_4 was prepared as previously described.[24] Anal. Calcd for $C_{25}H_{24}N_3O_6SClCu$: C, 50.59; H, 4.08; N, 7.08. Found: C, 50.24; H, 4.05; N, 6.88 (E&R Microanalytical Laboratory, Parsippany, NJ).

Safety note: Although no problems were encountered in working with perchlorate salts, these compounds are potentially hazardous and should be handled with care.

Spectrograde acetonitrile (Fisher Scientific, Fair Lawn, NJ) was used to prepare 1 mM solutions, which were degassed with nitrogen prior to each experiment. Recrystallized tetrabutylammonium perchlorate (TBAP) (Aldrich, Milwaukee, WI) was used as a supporting electrolyte (0.1 M).

Controlled Potential Coulometry and Spectroelectrochemistry. Electrochemical experiments were performed on a PAR potentiostat/galvanostat model 273 (Oak Ridge, TN). A 0.3 mM sample of Cu^{II}(**1**) was prepared with degassed acetonitrile containing 0.1 M TBAP. The reference electrode and a platinum coil working electrode (Bioanalytical Systems, West Lafayette, IN) were placed in the cell containing the sample. An electrolyte bridge was used to connect the setup to another cell, which contained a platinum foil counter electrode immersed in a 0.1 M TBAP solution in acetonitrile. The setup was assembled inside an Atmosbag glovebag (Aldrich, Milwaukee, WI), and a steady stream of argon was used to keep positive pressure in the system. A potential of −1 V was applied to the system while stirring, and the current decay was monitored to determine the end of electrolysis. The solution was then transferred to a CD or UV cell, and spectrophotometric measurements were performed (see below for CD procedures).

Cyclic Voltammetry. Experiments were performed using a BAS 100 B/W potentiostat (Bioanalytical Systems, West Lafayette, IN). A three-electrode cell was used inside a faraday cage, with a glassy-carbon working electrode (A = 0.07069 cm^2) (Bioanalytical Systems, West Lafayette, IN). A platinum wire (Aldrich, Milwaukee, WI) served as a counter electrode. The reference electrode was $Ag/AgClO_4$ (0.34 V vs SCE),[63] prepared from a piece of silver wire (Aldrich, Milwaukee, WI) electrooxidized overnight in 0.1 M TBAP (Aldrich, Milwaukee, WI) acetonitrile solution at 15 mA. The wire was encased in a glass tube fitted with a Vycor frit (Bioanalytical Systems, West Lafayette, IN) and filled with 0.5 M TBAP (Aldrich, Milwaukee, WI). Background subtraction was performed for each scan.

Curve Fitting. Electrochemical simulations were performed using DigiSim 3.03[44,61] (Bioanalytical Systems, West Lafayette, IN). Cyclic voltammograms were fitted assuming the square mechanism and Butler−Volmer kinetics for electron-transfer reactions. Under the CV parameters menu, "semi-infinite linear diffusion" was selected. To reduce the number of fitting parameters, initial fitting was carried out using approximate values of the standard potential ($E°$) evaluated from the experimental voltammogram, the transfer coefficient (α) was assumed to be 0.5, the homogeneous reaction parameters were assigned arbitrary values, and the diffusion coefficients of chemical species were assumed to be 10^{-6} cm^2 s^{-1}. The initial fit yielded approximate values of the standard potential and the rate constant for the reduction reaction and the diffusion coefficients. After the reduction peak shape was approximated, the oxidation peak shape was simulated. This process was repeated iteratively several times to obtain an acceptable fit. As the approximations became better, all other parameters were fitted, including α values, diffusion coefficients, and finally the homogeneous rate constants. The α values were in the range of 0.33−0.43 for the reduction cycle and 0.49−0.61 for the oxidation cycle; there were no apparent trends for the fitted values. The slight deviation from the theoretical value of 0.5 may be due to the complexity of our system. The electron-transfer rate constants were extracted after obtaining consistent parameter values for several scan rates.

SECM Setup and Procedure. Measurements were taken using a previously described instrument[62] in a feedback mode. A Teflon cell mounted on a vibration-free stage (Newport Corp., Fountain Valley, CA) served as the cell for SECM experiments. The working electrode was an 11 μm diameter carbon tip which was prepared by sealing carbon fibers (Amoco Performance Products, Greenville, SC) in glass as described previously.[57] A glassy-carbon electrode (A = 0.070 69 cm^2, Bioanalytical Systems, West Lafayette, IN) was used as the substrate electrode. The reference was a homemade $Ag/AgClO_4$ electrode described above. A flow of nitrogen was passed through the solution before each experiment to remove oxygen. During SECM measurements, the concentration of oxygen was kept low by creating a nitrogen blanket above the solution. The tip was polished before each experiment on 0.05 μm alumina on felt (Buehler, Ltd., Lake Bluff, IL). The instrument was shielded in a Faraday cage. The SECM procedure was described previously.[59]

Circular Dichroism. An Aviv 202 SF spectrophotometer equipped with an automatic titrator was utilized for the CD titration studies, with the sample compartment blanketed with a steady stream of nitrogen gas. Solutions were prepared in the glovebox using degassed acetonitrile. Absorption spectra were recorded on a Perkin-Elmer Lambda 5 spectrophotometer.

Synthesis. Characterizations were performed with a Varian Gemini 200 MHz spectrometer for ^{1}H and ^{13}C NMR, and a Bruker MALDI-TOF mass spectrometer was used with the matrix α-CHC to obtain mass spectra. Elemental analyses were performed by E&R Microanalytical Laboratories, Inc.

2-(Bis(quinolin-2-ylmethyl)amino)-4-(methylsulfinyl)butyric Acid, 2. To a stirring solution of 2-(bis(quinolin-2-ylmethyl)-amino)-4-(methylsulfanyl)butyric acid methyl ester[25] (1.94 g, 4.36 mmol) in 65 mL of 1:1 water/dichloromethane mixture was added bromine (224 μL, 4.36 mmol). After 24 h, the biphasic mixture was separated and the aqueous layer was neutralized with sodium bicarbonate and extracted with dichloromethane. The combined organic extracts were washed with brine, dried with $MgSO_4$, and evaporated. Purification was achieved by silica column chromatography, eluting the product with 5% methanol in dichloromethane (R_f = 0.31) to give 67% of the ester. Saponification was achieved by dissolving the ester (1.34 g, 2.9 mmol) in 8.6 mL of THF and stirring with an equal volume of 0.5 N LiOH for 2 h at ambient temperature. The mixture was evaporated to dryness and dissolved in water, which was acidified to pH 6.5 with perchloric acid. Extraction with dichloromethane and evaporation yielded crude

(61) Bott, A. W.; Feldberg, S. W.; Rudolph, M. *Curr. Sep.* **1996**, *15*, 67−71.
(62) Shao, Y.; Mirkin, M. V. *J. Phys. Chem. B* **1997**, *101*, 3202−3208.
(63) Zotti, G.; Zecchin, S.; Schiavon, G.; Louwet, F.; Groenendaal, L.; Crispin, X.; Osikowicz, W.; Salaneck, W.; Fahlman, M. *Macromolecules* **2003**, *36*, 3337−3344.

product, which was recrystallized from acetonitrile to give pure acid (421 mg, 32%). ^{1}H NMR (200 MHz, $CDCl_3$) [δ (ppm)]: 2.3−2.55 (m, 2H, sulfoxymethylene), 2.6 (s, 3H, sulfoxymethyl), 2.8−3.2 (m, 2H, methylene), 3.8−4.0 (m, 1H, methine), 4.3−4.4 (2s, 4H, quinoylmethylene), 7.3−8.2 (m, 12H, arom). ^{13}C NMR (50 MHz, $CDCl_3$) [δ (ppm)]: 22.79, 23.72, 38.88, 39.47, 51.69, 52.72, 57.01, 65.68, 66.09, 120.82, 127.21, 127.86, 128.12, 128.36, 130.63, 128.06, 147.03, 159.73, 175.18. MALDI (*m*/*e*): found, 448.4; calcd, 448.56 ($M + H^+$). Anal. Calcd for $C_{25}H_{25}N_3O_3S$: C, 67.09; H, 5.63; N, 9.42. Found: C, 67.29; H, 5.53; N, 9.42.

The complex Cu^{II}(**2**)(ClO_4) was obtained by adding $Cu(ClO_4)_2 \cdot 6H_2O$ (74.1 mg, 0.2 mmol) in 1 mL of MeOH to a stirring ligand (89.5 mg, 2 mmol) solution in 6 mL of methanol. The blue precipitate was collected and washed with ethyl ether (110 mg, 90.2%). MALDI (*m*/*e*): found, 511.0; calcd, 510.09 (M^+). Anal. Calcd for $C_{25}H_{24}ClCuN_3O_7S + H_2O$: C, 47.85; H, 4.18; N, 6.70. Found: C, 48.11; H, 3.66; N, 6.34.

Acknowledgment. We thank Prof. Nicholas Geacintov for insightful discussions on CD experiments. This project was funded by the National Science Foundation (Grants CHE-0316589 and CHE-0315558).

IC051048M